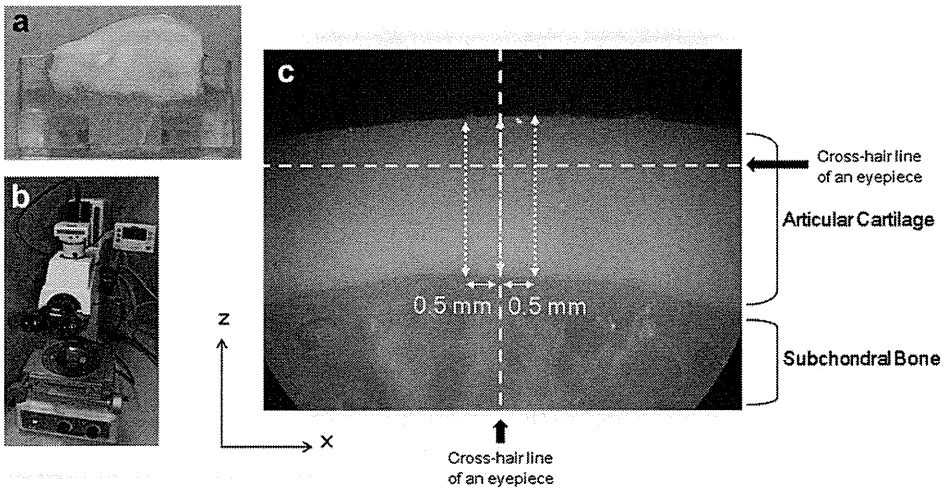

Fig. 5. Image showing (a) a cut osteochondral block fixed to a sample holder, (b) an optical measuring microscope and (c) cartilage thickness measurement using the microscope. The sample table of the microscope contained micrometers for sample position adjustment by parallel movement (x-z plane of the sample coordinate and sample rotation adjustment (θxz) in the horizontal plane. Cartilage thickness was measured along the z-axis direction at each line brightness data point by moving the crosshair pointer from the cartilage surface to the bone-cartilage interface.

corresponding to the B-mode ultrasound image plane. Subsequently, each sample was mounted on a glass slide, covered with a cover glass after dripping normal saline onto the sample surface to keep the cartilage moistened and inhibit deformation during measurement due to drying. Tc-optical was measured using an optical measuring microscope (× 30 magnification) (MM-400; Nikon, Tokyo, Japan) containing an eyepiece with adjustable crosshairs, with an adjustable stage system (MHS 2 × 2; Nikon) as the sample table. The adjustable stage contained two micrometers with a digital recorder for sample position adjustment by parallel movement (x-z plane of the sample coordinate) and a micrometer for sample rotation adjustment (θxz) in the horizontal plane (Fig. 5). With this optical measuring microscope and the stage, the sides of the sample holder, which were parallel to the direction of the ultrasound beam in acoustic signal acquisition, were aligned parallel to the direction of thickness measurement (z-axis direction of the sample coordinate). The center point of the sample holder was identified by measuring the distance from the sides of the sample holder (x-axis direction of the sample coordinate) and then the Tc-US measurement points on the cartilage surface were identified in a similar manner by measuring distance from the center point. Tc-optical along the beam direction (z-axis direction) was measured at each Tc-US measurement point by moving the crosshair pointer from the cartilage surface to the bone-cartilage interface.

Statistical analysis

Mean and standard deviation (SD) of Tc-US and Tc-optical for each sample were calculated. Linear regression analysis was performed and Pearson's correlation coefficient was used to compare Tc-US and Tc-optical. Statistical analysis was performed using SPSS Statistics version 17.0 software (SPSS, Chicago, IL), and results were considered significant for values of $p < 0.05$.

RESULTS

US images from conventional imaging and RTSCI are shown in Figure 6. With conventional US, the horizontal part of the cartilage surface was clear, whereas inclined parts were relatively blurred. With RTSCI, on the other hand, the whole cartilage surface was clear and the speckle and clutter seen on the cartilage and bone-cartilage border with conventional US was reduced.

In all B-mode line data, peaks of reflected ultrasound signals from the cartilage surface and cartilage-bone

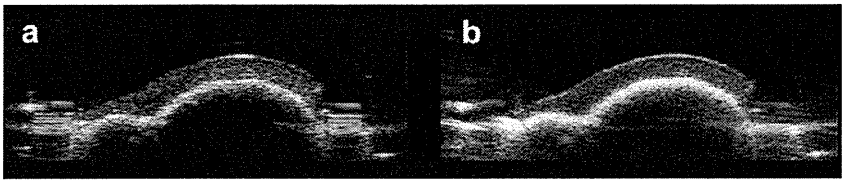

Fig. 6. B-mode US images of conventional imaging (a) and real-time spatial compound imaging (RTSCI) (b).

Table 1. Averages of articular cartilage thickness

	6-month-old pig	3-year-old pig
Tc-optical (mm)	2.40 ± 0.39	1.49 ± 0.10
Tc-US (conventional) (mm)	2.46 ± 0.42	1.45 ± 0.18
Tc-US (real-time spatial compound) (mm)	2.40 ± 0.47	1.47 ± 0.14

Values are presented as mean ± standard deviation.

border were clear enough to be identified. Mean (± standard deviation) Tc-optical and Tc-US (conventional, spatial compound) for both samples are shown in Table 1.

A significant linear correlation was seen between Tc-optical and Tc-US in conventional US (r = 0.961; 95% confidence interval, 0.936–0.976; root mean square error, 0.167 mm; $p < 0.0001$) (Fig. 7a). The slope was 1.08 with an intercept of −0.148 mm (not significantly different from 0, $p = 0.069$). A significant linear correlation was also noted between Tc-optical and Tc-US in RTSCI US (r = 0.976; 95% confidence interval, 0.961–0.985; root mean square error, 0.128 mm; $p < 0.0001$) (Fig. 7b). The slope was 1.06 with an intercept of −0.133 mm.

The accuracy of ultrasonographic measurement of Tc was studied using a Bland-Altman plot (Fig. 8). The mean differences between Tc-optical and Tc-US were −0.0073 mm and 0.0139 mm with standard deviations of 0.171 mm and 0.131 mm for conventional imaging and RTSCI, respectively.

DISCUSSION AND CONCLUSION

The purpose of this study was to measure the thickness of articular cartilage using B-mode imaging with a clinical US transducer and to assess the accuracy of measurements in comparison with optical measurement values. Among the past studies using A-mode US, Jurvelin et al. reported that the slope and intercept of the regression line for the relationship between optical and ultrasonic measurements were 0.849 and 0.104 mm, respectively (r = 0.905) (Jurvelin et al. 1995). The mean difference between optical and ultrasonic measurements was reportedly −0.0322 mm with a standard deviation of 0.164 mm. Toyras et al. reported that the mean difference between needle probe measurement and ultrasonic measurement was −0.002 mm with a standard deviation of 0.099 mm (Toyras et al. 2002). Suh et al. reported the slope and intercept of the regression line for the relationship between microscopic measurement and ultrasonic measurements with the in situ calibration method was 1.078 and −0.142 mm ($R^2 = 0.98$) (Suh et al. 2001). Conversely, Myers et al. performed a study on *in vitro* measurement of the thickness of human articular cartilage using B-mode US and reported a significant correlation between the histologic and US measurement values (r = 0.87) (Myers et al. 1995). That study, however, was performed with US at relatively high frequency (25 MHz). In our study using B-mode with a clinically applied frequency (10 MHz), the correlation coefficients between histologic and US measurement values were 0.961 and 0.976, and mean differences between Tc-optical and Tc-US were −0.0073 mm and 0.0139 mm with standard deviations of 0.171 mm and 0.131 mm for conventional imaging and RTSCI, respectively. These findings were not inferior to those obtained in previous studies, which have all been performed *in vitro*, including those with A-mode US.

One of the reasons behind the high accuracy of B-mode US measurements for articular cartilage in this study, we assume, was due to the method of determining the tissue border, which we defined as the brightness peaks of each reflected signal, whereas tissue borders

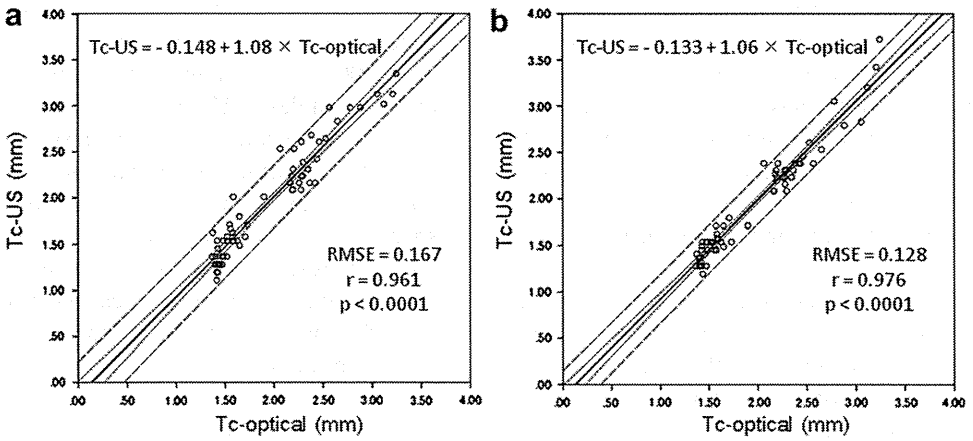

Fig. 7. Correlations between *Tc-optical* and *Tc-US* using samples from a 6-month-old pig and a 3-year-old pig. The 95% confidence intervals for regression (short dashes) and population (long dashes) for conventional imaging (a) and RTSCI (b) are shown. Root mean square errors (RMSE) and Pearson's correlation coefficients (r) are also shown.

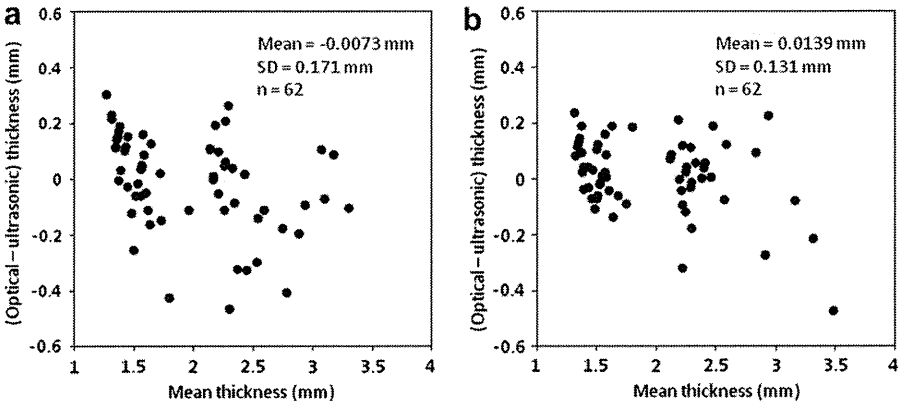

Fig. 8. Difference in cartilage thickness determined with ultrasound and microscopic techniques compared with mean thickness measured using ultrasound and microscopic techniques for conventional imaging (a) and RTSCI (b).

were positioned manually in the previous B-mode study (Myers et al. 1995). Even though manual segmentation is frequently performed clinically for B-mode images, such segmentation can be very subjective and dependent on the skill and experience of the examiner. Use of an objective method for determining cartilage surface and bone-cartilage interfaces could have affected the accuracy of thickness measurements for articular cartilage, which is a relatively thin tissue. Another reason for the high accuracy could have been the fine registration between Tc and Tc-US measurement points in this study. One of the obstacles to accurate assessment of Tc measurement using B-mode US is the technical difficulty of identifying the US scan plane and guaranteeing registration between the US scan plane and the histologic or optical evaluation plane. Having acknowledged this difficulty, we created an original setting for US image acquisition to gain US images running through the mid-center plane of the sample holder. In addition, we performed fine adjustment of US image orientation in extracting brightness line data for thickness measurements. With A-mode US, in general, thickness can be measured only on one point in one measurement. In the previous B-mode US study (Myers et al. 1995), B-mode images were created by moving the A-mode transducer and the range of assessment was 5 mm wide. We used a commercially available B-mode linear transducer and achieved highly accurate Tc-US measurement over a relatively wide range area (15 mm wide), possibly due to the reasons outlined above.

Although little difference was seen in the accuracy of thickness measurements for articular cartilage between conventional imaging and RTSCI, a quite clear difference in image quality was apparent. Lin et al. reported that RTSCI significantly improved the definition of soft-tissue planes, reduced speckle and other noise, and improved image detail when compared with conventional high-resolution sonography in a US study of the musculoskeletal system in 34 patients with lateral epicondylitis of the elbow, tears of the extremities or tendinopathy (Lin et al. 2002). Although RTSCI has been adopted for clinical evaluation of skeletal tissues, such as meniscus (Shanbhogue et al. 2009), tendon (Bartolotta et al. 2007; Entrekin et al. 2001), or ligament (Sorrentino et al. 2009) and has been reported to be useful, no studies have applied RTSCI for the evaluation of articular cartilage. According to our results, both conventional and RTSCI provide accurate measurement of Tc. In addition, RTSCI appears to have the potential to exhibit better images from the perspective of image quality and higher accuracy of Tc measurement than conventional US. We assume there are several reasons for the higher coefficient of correlation between Tc-US and Tc in RTSCI than in conventional US. First, speckle and clutter were reduced with RTSCI in our study, as reported in previous studies (Bartolotta et al. 2007; Lin et al. 2002; Shanbhogue et al. 2009). Speckle results from interference of acoustic fields generated by the scattering of the ultrasound beam from tissue reflectors, which is a random phenomenon and results in the characteristic grainy appearance of US images (Lin et al. 2002). By averaging the US images obtained from different angles of US beam, speckle can be reduced. In addition to speckle, noise could also be reduced by averaging the multiple image data and signal-to-noise ratio could be elevated by RTSCI. Second, the geographical shape of articular cartilage was assumed to have influenced the results with highly accurate RTSCI. To acquire clear US images of articular cartilage with conventional B-mode imaging, it is crucial that the US transducer be kept as orthogonal as possible to the cartilage surface (Barthez et al. 2007). However, the cartilage surface generally has an uneven topography and acquisition of a uniform brightness border either at the cartilage surface or at the bone-cartilage interface over a wide area is difficult. Under such conditions, improved image quality

could be obtained by RTSCI, which reduces the angle-dependency of detection of the articular cartilage surface and bone-cartilage interface. In fact, measurement of Tc in this study was performed under idealized conditions, including a relatively orthogonal imaging plane with a set focus distance. However, we believe that the features of RTSCI can contribute to improved tissue-plane definition and image quality in clinical applications. In addition, although potentially representing only a small difference for an experienced clinician or sonographer performing manual measurement, we think these benefits of RTSCI could be valuable in clinical measurement. In particular, an objective method for determining cartilage surface and bone-cartilage interfaces that could be applied to achieve high accuracy and repeatability in Tc measurements to reduce intra- and interobserver error would be indispensable for longitudinal evaluations of OA patients, since articular cartilage is relatively thin.

Several limitations to the present study must be kept in mind. Tc measurement using US was carried out *in vitro*, whereas we are aiming toward clinical measurement of Tc using US. One reason we performed Tc measurement *in vitro* was that acquiring the position and orientation of the US B-mode scan plane is technically very difficult *in vivo* and performing accuracy assessment by obtaining the same plane for Tc measurement would, thus, be infeasible. Myers et al. carried out Tc measurements using B-mode slice images of human femoral osteochondral blocks from an OA patient in a water tank with a 25-MHz US linear transducer, where both ends of the scan plane were marked with ink, then compared measured values with Tc measured using a histologic section created with a scalpel blade, finding a good relationship with a correlation coefficient of 0.87 (Myers et al. 1995). Our study identified the US plane position and orientation by acquisition of the US image in the plane containing certain known points, then created a cut of the corresponding plane for Tc measurement of accuracy using a diamond saw device. With this procedure, we assume that we achieved very accurate registration between the US scan plane and cut plane, which is crucial for accuracy assessment. However, for further evaluations of accuracy, Tc-US measurements on cadavers or preoperative patients and histologic or optical Tc measurements of extracted osteochondral blocks should be performed with registration, if possible. Another limitation was that the US device only allowed us to perform RTSCI with three frames. Theoretically, reduction of speckle and noise could be enhanced with a greater number of frames compounded when the speckle patterns are uncorrelated (Trahey et al. 1986) among the images acquired by different US beam angles. On the other hand, one of the main limitations of spatial compounding in clinical use is the increased time requirement for a cycle of US beam steering and a resulting persistence effect when the object includes movement (Sorrentino et al. 2009). However, we assume that this persistence effect would not occur if the target extremity was fixed and did not move. In fact, Leotta et al. performed 3-D spatial compounding with ultrasound imaging of the shoulder rotator cuff on supine volunteers using a US transducer mounted with a magnetic transmitter, reconstructed multiple converted images to 3-D compound volume data, measured rotator cuff thickness and achieved relatively high precision of 0.08 mm for mean differences among multiple measurements (Leotta and Martin 2000). A greater number of frames in compounding could, thus, be appropriate and should be considered in the future, even though we achieved very high accuracy of Tc measurement with RTSCI averaged from three frames. The last limitation was that we applied different speeds of sound determined in a previous study to each sample cartilage to achieve accurate measurement of Tc. The speed of sound in cartilage is usually calculated *in vitro* from time of flight by US traveling through cartilage and Tc measured by a needle probe, which could be invasive to cartilage (Jurvelin et al. 1995; Nieminen et al. 2002). With a special device, Nieminen et al. applied mechanical load on extracted cartilage samples and calculated speed of sound from time of flight and displacement of the probe (Nieminen et al. 2007). In clinical situations, however, measuring the speed of sound in articular cartilage is technically difficult. Toyras et al. used bovine cartilage samples from healthy degenerated parts and reported the speed of sound ranged from 1555 m/s to 1685 m/s (Toyras et al. 2003). They performed indentation tests and created simulation curves for the relationships among speed of sound, thickness and error in the modulus of cartilage, revealing that a constant speed of sound can be utilized to obtain clinically acceptable accuracy for cartilage thickness. The ideal would be to measure the speed of sound *in vivo*, although a constant speed of sound would presumably provide relatively accurate values in clinical measurement of Tc by B-mode US imaging.

This study was performed under idealized conditions, which includes the *in vitro* setting. Based on our results, we assume an objective method for determining cartilage surface and bone-cartilage interfaces along with spatial compound imaging would enable clinical measurement of cartilage thickness, possibly with high accuracy and repeatability. We also assume that some adjustment would be necessary for the cartilage surface determination algorithm in clinical applications, due to the presence of soft tissues between the cartilage and US linear transducer surface. Clinical usage would be limited to specific locations where the cartilage surface can be considered relatively orthogonal to the US beam,

such as the distal femoral condyle with knee flexed. With spatial compound imaging and refinement of the tissue border determination algorithm, however, the potential locations for application would expand.

In summary, we undertook measurement of articular cartilage thickness *in vitro* using both conventional and real-time spatial compound B-mode US with a clinical transducer to evaluate the accuracy of measurement. From our results, RTSCI may offer higher accuracy for measuring Tc than conventional methods, even though both showed good accuracy in our study. We believe the accuracy of our method is sufficiently high to allow application to measurement of human Tc in future studies.

Acknowledgments—This work was funded by a grant-in-aid (Comprehensive Research on Aging and Health H19-007) as a Health and Labour Sciences Research Grant from the Ministry of Health, Labour and Welfare of Japan. The authors wish to thank Mr. Koichi Miyasaka and Mr. Ryoichi Sakai from the Research Laboratory at Aloka Co. Ltd. (Tokyo, Japan) for their technical support.

REFERENCES

Adam C, Eckstein F, Milz S, Schulte E, Becker C, Putz R. The distribution of cartilage thickness in the knee-joints of old-aged individuals–Mmeasurement by A-mode ultrasound. Clin Biomech (Bristol, Avon) 1998;13:1–10.

Aisen AM, McCune WJ, MacGuire A, Carson PL, Silver TM, Jafri SZ, Martel W. Sonographic evaluation of the cartilage of the knee. Radiology 1984;153:781–784.

Barthez PY, Bais RJ, Vernooij JC. Effect of ultrasound beam angle on equine articular cartilage thickness measurement. Vet Radiol Ultrasound 2007;48:457–459.

Bartolotta TV, Taibbi A, Malizia G, Mamone G, Barbagallo C, Midiri M, Lagalla R. Real-time spatial compound sonography of Achilles tendon in patients with heterozygous familial hypercholesterolaemia and normal physical examination. Radiol Med 2007;112:562–571.

Carpenter DA, Dadd MJ, Kossoff G. A multimode real time scanner. Ultrasound Med Biol 1980;6:279–284.

Castriota-Scanderbeg A, De Micheli V, Scarale MG, Bonetti MG, Cammisa M. Precision of sonographic measurement of articular cartilage: Inter- and intraobserver analysis. Skeletal Radiol 1996; 25:545–549.

Cha JH, Moon WK, Cho N, Chung SY, Park SH, Park JM, Han BK, Choe YH, Cho G, Im JG. Differentiation of benign from malignant solid breast masses: Conventional US versus spatial compound imaging. Radiology 2005;237:841–846.

Cherin E, Saied A, Laugier P, Netter P, Berger G. Evaluation of acoustical parameter sensitivity to age-related and osteoarthritic changes in articular cartilage using 50-MHz ultrasound. Ultrasound Med Biol 1998;24:341–354.

Chiang EH, Adler RS, Meyer CR, Rubin JM, Dedrick DK, Laing TJ. Quantitative assessment of surface roughness using backscattered ultrasound: The effects of finite surface curvature. Ultrasound Med Biol 1994;20:123–135.

Eckstein F, Buck RJ, Burstein D, Charles HC, Crim J, Hudelmaier M, Hunter DJ, Hutchins G, Jackson C, Kraus VB, Lane NE, Link TM, Majumdar LS, Mazzuca S, Prasad PV, Schnitzer TJ, Taljanovic MS, Vaz A, Wyman B, Le Graverand MP. Precision of 3.0 Tesla quantitative magnetic resonance imaging of cartilage morphology in a multicentre clinical trial. Ann Rheum Dis 2008; 67:1683–1688.

Eckstein F, Hudelmaier M, Wirth W, Kiefer B, Jackson R, Yu J, Eaton CB, Schneider E. Double echo steady state magnetic resonance imaging of knee articular cartilage at 3 Tesla: A pilot study for the Osteoarthritis Initiative. Ann Rheum Dis 2006;65:433–441.

Eckstein F, Kunz M, Schutzer M, Hudelmaier M, Jackson RD, Yu J, Eaton CB, Schneider E. Two year longitudinal change and test-retest-precision of knee cartilage morphology in a pilot study for the osteoarthritis initiative. Osteoarthritis Cartilage 2007;15: 1326–1332.

Entrekin RR, Porter BA, Sillesen HH, Wong AD, Cooperberg PL, Fix CH. Real-time spatial compound imaging: Application to breast, vascular, and musculoskeletal ultrasound. Semin Ultrasound CT MR 2001;22:50–64.

Huber S, Wagner M, Medl M, Czembirek H. Real-time spatial compound imaging in breast ultrasound. Ultrasound Med Biol 2002;28:155–163.

Jespersen SK, Wilhjelm JE, Sillesen H. Multi-angle compound imaging. Ultrason Imaging 1998;20:81–102.

Jespersen SK, Wilhjelm JE, Sillesen H. *In vitro* spatial compound scanning for improved visualization of atherosclerosis. Ultrasound Med Biol 2000;26:1357–1362.

Jurvelin JS, Rasanen T, Kolmonen P, Lyyra T. Comparison of optical, needle probe and ultrasonic techniques for the measurement of articular cartilage thickness. J Biomech 1995;28:231–235.

Kaleva E, Saarakkala S, Toyras J, Nieminen HJ, Jurvelin JS. *In vitro* comparison of time-domain, frequency-domain and wavelet ultrasound parameters in diagnostics of cartilage degeneration. Ultrasound Med Biol 2008;34:155–159.

Kane D, Balint PV, Sturrock R, Grassi W. Musculoskeletal ultrasound–A state of the art review in rheumatology. Part 1: Current controversies and issues in the development of musculoskeletal ultrasound in rheumatology. Rheumatology (Oxford) 2004;43:823–828.

Kellgren JH, Lawrence JS. Radiological assessment of osteo-arthrosis. Ann Rheum Dis 1957;16:494–502.

Kofoed SC, Gronholdt ML, Wilhjelm JE, Bismuth J, Sillesen H. Real-time spatial compound imaging improves reproducibility in the evaluation of atherosclerotic carotid plaques. Ultrasound Med Biol 2001;27:1311–1317.

Leotta DF, Martin RW. Three-dimensional ultrasound imaging of the rotator cuff: Spatial compounding and tendon thickness measurement. Ultrasound Med Biol 2000;26:509–525.

Lin DC, Nazarian LN, O'Kane PL, McShane JM, Parker L, Merritt CR. Advantages of real-time spatial compound sonography of the musculoskeletal system versus conventional sonography. AJR Am J Roentgenol 2002;179:1629–1631.

McCune WJ, Dedrick DK, Aisen AM, MacGuire A. Sonographic evaluation of osteoarthritic femoral condylar cartilage. Correlation with operative findings. Clin Orthop Relat Res 1990;230–235.

Moller B, Bonel H, Rotzetter M, Villiger PM, Ziswiler HR. Measuring finger joint cartilage by ultrasound as a promising alternative to conventional radiograph imaging. Arthritis Rheum 2009;61:435–441.

Multanen J, Rauvala E, Lammentausta E, Ojala R, Kiviranta I, Hakkinen A, Nieminen MT, Heinonen A. Reproducibility of imaging human knee cartilage by delayed gadolinium-enhanced MRI of cartilage (dGEMRIC) at 1.5 Tesla. Osteoarthritis Cartilage 2009;17:559–564.

Myers SL, Dines K, Brandt DA, Brandt KD, Albrecht ME. Experimental assessment by high frequency ultrasound of articular cartilage thickness and osteoarthritic changes. J Rheumatol 1995;22:109–116.

Naredo E, Cabero F, Palop MJ, Collado P, Cruz A, Crespo M. Ultrasonographic findings in knee osteoarthritis: A comparative study with clinical and radiographic assessment. Osteoarthritis Cartilage 2005; 13:568–574.

Nieminen HJ, Julkunen P, Toyras J, Jurvelin JS. Ultrasound speed in articular cartilage under mechanical compression. Ultrasound Med Biol 2007;33:1755–1766.

Nieminen HJ, Toyras J, Rieppo J, Nieminen MT, Hirvonen J, Korhonen R, Jurvelin JS. Real-time ultrasound analysis of articular cartilage degradation in vitro. Ultrasound Med Biol 2002;28: 519–525.

Ohashi S, Ohnishi I, Matsumoto T, Matsuyama J, Bessho M, Tobita K, Kaneko M, Nakamura K. Comparison of ultrasound speed in articular cartilage measured by different time-of-flight methods. J Med Ultrason 2011;38:225–234.

Oktar SO, Yucel C, Ozdemir H, Uluturk A, Isik S. Comparison of conventional sonography, real-time compound sonography, tissue

harmonic sonography, and tissue harmonic compound sonography of abdominal and pelvic lesions. AJR Am J Roentgenol 2003;181: 1341–1347.

Peterfy C, Kothari M. Imaging osteoarthritis: Magnetic resonance imaging versus x-ray. Curr Rheumatol Rep 2006;8:16–21.

Shanbhogue AK, Sandhu MS, Singh P, Ojili V, Khandelwal N, Sen R. Real-time spatial compound ultrasound in the evaluation of meniscal injuries: A comparison study with conventional ultrasound and MRI. Knee 2009;16:191–195.

Shapiro RS, Simpson WL, Rausch DL, Yeh HC. Compound spatial sonography of the thyroid gland: Evaluation of freedom from artifacts and of nodule conspicuity. AJR Am J Roentgenol 2001;177:1195–1198.

Shattuck DP, von Ramm OT. Compound scanning with a phased array. Ultrason Imaging 1982;4:93–107.

Sorrentino F, Iovane A, Nicosia A, Candela F, Midiri M, Lagalla R. Role of high-resolution ultrasonography without and with real-time spatial compound imaging in evaluating the injured posterior cruciate ligament: Preliminary study. Radiol Med 2009;114:312–320.

Suh JK, Youn I, Fu FH. An *in situ* calibration of an ultrasound transducer: A potential application for an ultrasonic indentation test of articular cartilage. J Biomech 2001;34:1347–1353.

Toyras J, Laasanen MS, Saarakkala S, Lammi MJ, Rieppo J, Kurkijarvi J, Lappalainen R, Jurvelin JS. Speed of sound in normal and degenerated bovine articular cartilage. Ultrasound Med Biol 2003;29:447–454.

Toyras J, Nieminen HJ, Laasanen MS, Nieminen MT, Korhonen RK, Rieppo J, Hirvonen J, Helminen HJ, Jurvelin JS. Ultrasonic characterization of articular cartilage. Biorheology 2002;39: 161–169.

Trahey GE, Smith SW, von Ramm OT. Speckle pattern correlation with lateral aperture translation: Experimental results and implications for spatial compounding. IEEE Trans Ultrason Ferroelectr Freq Control 1986;33:257–264.

Wang SZ, Huang YP, Saarakkala S, Zheng YP. Quantitative assessment of articular cartilage with morphologic, acoustic and mechanical properties obtained using high-frequency ultrasound. Ultrasound Med Biol 2010;36:512–527.

Wortsman XC, Holm EA, Wulf HC, Jemec GB. Real-time spatial compound ultrasound imaging of skin. Skin Res Technol 2004;10: 23–31.

Yen CL, Chang HY, Huang SY, Huang YC, Jeng CM. Combination of tissue harmonic sonography, real-time spatial compound sonography and adaptive image processing technique for the detection of carotid plaques and intima-medial thickness. Eur J Radiol 2009;71:11–16.

Yen CL, Jeng CM, Yang SS. The benefits of comparing conventional sonography, real-time spatial compound sonography, tissue harmonic sonography, and tissue harmonic compound sonography of hepatic lesions. Clin Imaging 2008;32:11–15.

Geriatrics Gerontology 1st Impact Factor in June 2010 Medline Indexed

Geriatr Gerontol Int 2012; **12:** *652–658*

ORIGINAL ARTICLE: EPIDEMIOLOGY, CLINICAL PRACTICE AND HEALTH

Estimation of appendicular muscle mass and fat mass by near infrared spectroscopy in older persons

Daisuke Yoshida,[1] Hiroyuki Shimada,[1] Atsushi Harada,[2] Yasumoto Matsui,[2] Yoshihito Sakai[2] and Takao Suzuki[3]

[1]Section for Health Promotion, Department of Health and Medical Care, Center for Development of Advanced Medicine for Dementia, [2]Department of Orthopedic Surgery, National Hospital for Geriatric Medicine, and [3]Research Institute, National Center for Geriatrics and Gerontology, Obu, Aichi, Japan

Aim: Near infrared spectroscopy has been reported to have a high reliability and accuracy in assessing the percentage of body fat. However, whether muscle mass can be accurately estimated using this method has not been established. This study examined whether a near infrared spectroscopy method could estimate appendicular muscle mass and fat mass, with dual-energy X-ray absorptiometry as the standard method for comparison.

Methods: A total of 20 orthopedic inpatients (mean age 73.2 ± 6.8 years) were recruited for this study. Their body composition was assessed using near infrared spectroscopy and dual-energy X-ray absorptiometry. Appendicular muscle mass and fat mass were estimated from height, weight and optical densities.

Results: The optical densities for the upper arm (biceps, triceps) and forearm (flexor carpi radialis) were significantly correlated with appendicular muscle mass ($r = 0.534$ to 0.623) or fat mass ($r = -0.483$ to -0.827). Estimated appendicular muscle mass and fat mass explained 89% and 80% of the variance in the dual-energy X-ray absorptiometry-derived muscle mass and fat mass estimates using height, weight and optical density values of the proximal flexor carpi radialis.

Conclusions: Near infrared spectroscopy is a useful method to assess not only fat mass, but also muscle mass in older adults. **Geriatr Gerontol Int 2012; 12: 652–658.**

Keywords: aged, body composition, body fat, sarcopenia, skeletal muscles.

Introduction

Age-related loss of muscle mass (so-called sarcopenia) can lead to functional decline in older persons.[1–5] Two published Health, Aging and Body Composition reports showed that sarcopenia, as determined by computed tomography (CT) in the mid-thigh, was a weak to modest predictor of loss of physical function over the following 2 to 3 years.[6,7] Furthermore, one study reported that older sarcopenic patients were twice as likely to contract infection during a hospital stay compared with older patients with a normal muscle mass.[8] This suggested that sarcopenic individuals might have decreased immunity, which might provide a mechanistic link between sarcopenia and mortality risk. In addition, reduced arm muscle area was reported to be an independent predictor of long-term mortality in community-dwelling older adults.[9] According to the

Accepted for publication 27 December 2011.

Correspondence: Dr Daisuke Yoshida PhD, Section for Health Promotion, Department of Health and Medical Care, Center for Development of Advanced Medicine for Dementia, National Center for Geriatrics and Gerontology, 35 Gengo, Morioka-machi, Obu, Aichi 474-8511, Japan.
Email: yoshida@ncgg.go.jp

New Mexico Elder Health Survey, the prevalence of sarcopenia increased from 13 to 24% in persons aged under 70 years to >50% in persons aged over 80 years.[1] To achieve successful aging, it is important to preserve muscle mass to maintain function.

Recently, some researchers reported that sarcopenic patients who were obese were at particularly high risk of functional impairment and physical disability.[10–13] The condition was termed sarcopenic obesity, and it was suggested that approximately 15% of those with sarcopenia were also obese.[10] This suggests that it is necessary to assess not only muscle mass, but also fat mass accurately in the elderly.

There are various methods for measurement of body composition. Total body and regional skeletal muscle mass can now be accurately quantified using imaging methods, including CT and magnetic resonance imaging (MRI).[14] However, CT and MRI are costly methods and access to the equipment can be limited. Dual-energy X-ray absorptiometry (DXA) has been widely used in clinical practice, not only for osteoporosis screening and diagnosis, but also for assessment of body composition, such as skeletal muscle mass and fat mass. DXA is less expensive and less invasive compared with MRI and CT. Previous studies have shown good correlations between DXA-derived lean soft tissue mass and skeletal muscle mass in the lower limb region when CT and MRI were used as the standards for comparison.[15,16] However, DXA methods take more time, although whole-body scanning by this method exposes the patient to minimal radiation.

Bioelectrical impedance analysis (BIA) is a non-invasive, portable, quick and inexpensive method for measuring body composition.[17] Previous studies have shown that there is a strong correlation between BIA resistance and skeletal muscle measurements in the arms[18] and legs.[19] In addition, one report suggested that BIA could provide rapid and accurate estimates of whole body skeletal muscle mass in adults.[20] There are some disadvantages with the BIA method. First, fat tissue also holds water, although the proportion is small.[21] Second, the volume of muscle derived by BIA might overestimate the actual volume. Third, there are a large proportion of older adults who have a changed distribution of body water, such as edema. One report showed that the expansion of extracellular water relative to intracellular water and to regional lean volume masks actual muscle cell atrophy during aging.[22] This suggested that it might be difficult to accurately assess body composition in older adults.

Another development that might have potential for use in older adults is near infrared spectroscopy (NIRS). NIRS is also a non-invasive, simple and rapid method of assessing the percentage of body fat. There are some reports that the NIRS method has a high reliability and accuracy in determination of the percentage of body fat.[23–25] In contrast, it has not been established whether muscle mass can be estimated accurately by NIRS.

The present study investigated whether a NIRS method could provide an accurate estimate of appendicular muscle mass (AMM) and appendicular fat mass (AFM) using DXA as the standard method for comparison.

Methods

Participants

A total of 20 orthopedic patients who were admitted to the National Hospital for Geriatric Medicine and who were aged 60 years or older were recruited for the present study. Patients with dementia or who had major laterality of muscle mass in the arms and legs, or who had surgery just before the study were excluded. All participants had their height (to the nearest 0.1 cm) and weight (to the nearest 0.1 kg) measured after admission. The details of the study were explained in advance and written consent was obtained from each participant. In addition, the present study was approved by the ethics committee of the National Center for Geriatrics and Gerontology.

Measurement of body composition

Whole and regional body composition was measured using DXA (Lunar DPX, Madison, WI, USA). This system provided the mass of lean soft tissue, fat and bone mineral for both the whole body and specific regions. Appendages were isolated from the trunk and head by using a DXA regional computer-generated default line. AMM or AFM was derived as the sum of the fat-free soft tissues or fat tissue of the arms and legs. A previous study reported that total body skeletal muscle mass can be accurately predicted from DXA-estimated appendicular lean soft tissue mass.[26,27]

NIRS

The NIRS measurements were carried out with the Fitness Analyzer BFT-3000 (Kett Electrical Laboratory, Tokyo, Japan, Fig. 1), the Japanese version of the Futrex 5000 (Futrex, Gaithersburg, MD, USA; 1988), which has potential for estimating body composition.[22,28] This device uses optical densities (OD) at two wavelengths (OD1 = 937 nm, OD2 = 947 nm) measured at each site. The NIRS instrument was tested immediately before taking measurements on each patients by using an optical standard, which was provided with the instrument and situated in a flexible light shield, to ensure that its performance was consistent throughout the study.

OD values were obtained at six sites: distal biceps (5 cm from the olecranon), distal triceps (5 cm from the

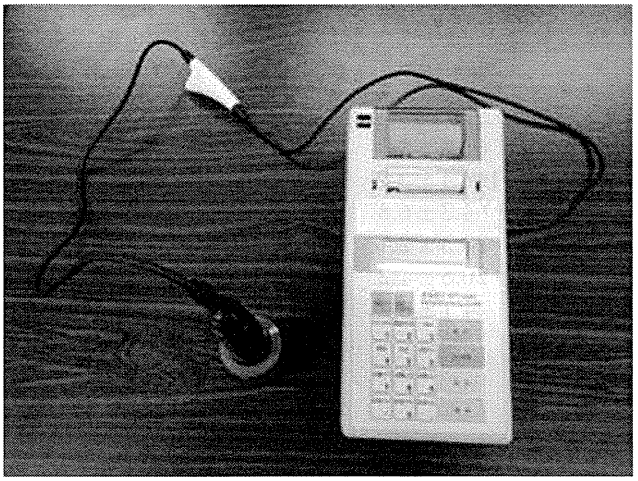

Figure 1 The near infrared spectroscopy instrument (Fitness Analyzer BFT-3000).

Figure 2 Method of measurement.

olecranon), proximal flexor carpi radialis (5 cm from the olecranon), distal quadriceps (5 cm from the upper edge of patella), proximal tibialis anterior (5 cm from the caput fibulae) and proximal calf (5 cm from the caput fibulae). The reliability was confirmed by test–retest. The test–retest reproducibility was excellent (intraclass correlation coefficient = 0.95–0.97, $P < 0.01$). Patients were required to maintain a seated position, with their arms relaxed at their sides (Fig. 2). NIRS measurements were carried out by a single trained physical therapist, and completed within a few minutes.

Statistical analysis

Pearson's correlation coefficient was used to determine the relationship between AMM or AFM and each OD value. Equations for estimation of AMM and AFM were developed with the use of multiple linear regression analysis. Potential explanatory variables included OD value, height and weight. DXA-measured AMM and AFM were set as the objective variable. The coefficient of determination (R^2) values were used to quantify the accuracy of model fit. The mean difference between DXA-measured AMM (AFM) and estimated AMM (AFM) was tested using the paired Student's *t*-test. Statistical analyses were carried out using PASW Statistics 18 for Windows (SPSS, Chicago, IL, USA) and the significance level was less than 5%.

Results

The characteristics of the patients are shown in Table 1. Mean age was 73.2 ± 6.8 years (range 62–84 years) and 70% were female. The subjects were diagnosed with the following: spinal canal stenosis ($n = 11$), disc herniation ($n = 1$), spinal tumor ($n = 2$), knee osteoarthritis ($n = 2$), compression fracture ($n = 1$), femoral neck fracture ($n = 1$) and others ($n = 2$).

The correlation coefficients between AMM or AFM and each OD value are listed in Table 2. AMM was significantly correlated with OD values at the distal triceps (OD1: $r = 0.623$; OD2: $r = 0.534$). AFM was significantly correlated with OD values at the distal biceps (OD1 $r = -0.570$; OD2 $r = -0.551$), distal triceps (OD1 $r = -0.483$; OD2 $r = -0.494$) and proximal flexor carpi radialis (OD1 $r = -0.827$; OD2 $r = -0.821$). In the correlation analysis between muscle mass or fat mass and the OD value, correlation coefficients were mostly higher with OD1 than with OD2. Thus, OD1 was used as the representative value of NIRS data for the estimation equation.

The results from linear regression analyses for the multivariate models are presented in Table 3. The multiple regression equations incorporated height, weight and OD1. Using anthropometric data (height and weight) as the explanatory variables, the R^2 value of AMM and AFM were 0.81 (standard error of the estimate [SEE] = 1.67 kg) and 0.50 (SEE = 1.77 kg), respectively (model 1). When OD1 was added to the explanatory variables, the R^2 values of AMM and AFM ranged from 0.85 to 0.89, and 0.58 to 0.80, respectively (models 2–5). The highest R^2 values of AMM and AFM were 0.89 (SEE = 1.33 kg) and 0.80 (SEE = 1.16 kg), respectively, when OD1 at the proximal flexor carpi radialis was added to the explanatory variables. For separate estimation equations (upper and lower limb), the accuracy of model fit was slightly less (muscle mass $R^2 = 0.82$–0.87, fat mass $R^2 = 0.53$–0.55). There were no significant differences between DXA-measured AMM and estimated AMM (mean difference 0.01, 95% confidence interval −0.56 to 0.58), or between DXA-measured AFM and estimated AFM (mean difference −0.25, 95% confidence interval −0.75 to 0.25).

Table 1 Physical characteristics of the study participants

Variables	All subjects ($n = 20$)	Men ($n = 6$)	Women ($n = 14$)
Age (years)	73.2 ± 6.8	67.8 ± 8.1	75.5 ± 4.9
Height (cm)	153.2 ± 9.5	166.1 ± 3.2	147.8 ± 4.3
Weight (kg)	53.9 ± 10.3	64.3 ± 6.8	49.4 ± 8.2
BMI (kg/m^2)	22.8 ± 2.9	23.3 ± 2.1	22.6 ± 3.2
AMM (kg)	15.7 ± 3.7	20.5 ± 1.2	13.6 ± 2.0
AFM (kg)	4.8 ± 2.4	4.1 ± 2.2	5.1 ± 2.4
Diagnosis n (%)			
Spinal canal stenosis	11 (55%)		
Disc herniation	1 (5%)		
Spinal tumor	2 (10%)		
Knee osteoarthritis	2 (10%)		
Compression fracture	1 (5%)		
Femoral neck fracture	1 (5%)		
Others	2 (10%)		

Values are mean ± standard deviation or n (%).
AFM, dual-energy X-ray absorptiometry-derived appendicular fat mass; AMM, dual-energy X-ray absorptiometry-derived appendicular muscle mass; BMI, body mass index.

Table 2 Correlation coefficients between limb muscle mass or fat mass and each optical densities value

	Biceps		Triceps		Flexor carpi radialis	
	OD1	OD2	OD1	OD2	OD1	OD2
Upper limb muscle mass						
Four limbs	0.369	0.350	0.623**	0.534*	0.343	0.324
Upper limb	0.292	0.286	0.572**	0.462*	0.279	0.267
Upper limb fat mass						
Four limbs	−0.570**	−0.551*	−0.483*	−0.494*	−0.827**	−0.821**
Upper limb	−0.423	−0.394	−0.403	−0.411	−0.723**	−0.705**
	Quadriceps		Tibialis anterior		Calf	
	OD1	OD2	OD1	OD2	OD1	OD2
Lower limb muscle mass						
Four limbs	0.332	0.190	0.139	0.118	0.297	0.327
Lower limb	0.383	0.248	0.138	0.125	0.346	0.373
Lower limb fat mass						
Four limbs	−0.348	−0.220	−0.421	−0.388	−0.426	−0.443
Lower limb	−0.333	−0.218	−0.434	−0.401	−0.458*	−0.472*

*$P < 0.05$; **$P < 0.01$. Optical density (OD)1 = 937 nm, OD2 = 947 nm.

Discussion

Recently, Sanada *et al.* reported prediction models for skeletal muscle index using body mass index (BMI) in Japanese adults.[29] The results showed that the R^2 values for the skeletal muscle index were 0.56 in men and 0.45 in women. Similarly, Gallagher *et al.* reported that height and weight accounted for 64% and 67% of the total variance of the appendicular skeletal muscle mass in African-American and Caucasian women, respectively, and 63% and 39% of the total variance in African-American and Caucasian men, respectively.[30] These results showed the difficulty in estimating the AMM accurately using only anthropometric measurements, and the need for an objective method for accurate measurement of body composition.

To address this problem, we investigated whether AMM and AFM could be estimated by a combination of height, weight and NIRS data (OD values). The present results showed that OD1 of the proximal flexor carpi

Table 3 Regression equation for estimating appendicular muscle mass and fat mass

Model	Equation	R^2	SEE
Appendicular muscle mass			
1	$y = 0.23 \times$ (height) $+ 0.13 \times$ (weight) $- 26.35$	0.81	1.67
2	$y = 0.17 \times$ (height) $+ 0.17 \times$ (weight) $+ 8.45 \times$ [OD1 [biceps]) $- 28.97$	0.89	1.34
3	$y = 0.13 \times$ (height) $+ 0.18 \times$ (weight) $+ 10.49 \times$ (OD1 [triceps]) $- 23.19$	0.85	1.55
4	$y = 0.10 \times$ (height) $+ 0.24 \times$ (weight) $+ 7.82 \times$ (OD1 [flexor carpi radialis]) $- 21.42$	0.89	1.33
5	$y = 0.20 \times$ (height) $+ 0.15 \times$ (weight) $+ 6.12 \times$ (OD1 [calf]) $- 29.44$	0.85	1.57
Appendicular fat mass			
1	$y = -0.22 \times$ (height) $+ 0.25 \times$ (weight) $+ 25.39$	0.50	1.77
2	$y = -0.17 \times$ (height) $+ 0.21 \times$ (weight) $- 7.89 \times$ (OD1 [biceps]) $+ 27.84$	0.65	1.52
3	$y = -0.10 \times$ (height) $+ 0.20 \times$ (weight) $- 12.11 \times$ (OD1 [triceps]) $+ 21.73$	0.61	1.60
4	$y = -0.06 \times$ (height) $+ 0.12 \times$ (weight) $- 10.01 \times$ (OD1 [flexor carpi radialis]) $+ 19.08$	0.80	1.16
5	$y = -0.19 \times$ (height) $+ 0.23 \times$ (weight) $- 6.55 \times$ (OD1 [calf]) $+ 28.70$	0.58	1.66

R^2, coefficient of determination; SEE, standard error of the estimate.

radialis, in association with anthropometric data, can provide accurate estimates of both AMM and AFM in older adults, although the NIRS data alone did not reflect muscle mass except at the distal triceps. Furthermore, compared with the estimation equation that included only anthropometric data, the estimation equation that included both anthropometric and NIRS data had a higher coefficient of determination.

In the present study, the NIRS data were obtained at six sites to determine the best location for estimating AMM and AFM. As a result, OD values measured at the distal triceps and proximal flexor carpi radialis showed a good correlation coefficient with limb muscle mass and fat mass, respectively. Yasukawa *et al.* reported that the NIRS data (OD values) measured by BFT-2000 (old model of BFT-3000) had higher correlations with percentage fat at the thinner adipose sites than thicker adipose sites,[31] and similar results were observed by Futrex 5000 in another report.[25] Inconsistent strengths of the association of OD values with total body fat at the various sites might simply be a result of differences in the depth of penetration of the infrared radiation. These results suggested that it might be preferable to carry out measurements at sites where there is little subcutaneous fat, such as the flexor carpi radialis.

There are several reports of NIRS being a valid method to assess the percentage of fat or fat mass. For example, Sawai *et al.* reported that the correlation coefficient between percentage body fat as predicted by the NIRS method and as predicted by the hydrostatic weighing technique was 0.88 ($P < 0.001$, SEE = 3.2).[24] Fuller *et al.* also suggested that NIRS methods using Futrex 5000 have the potential to replace skinfold thickness (SFT) for estimation of body composition.[25] The BFT-3000 used in the present study was developed for Japanese patients, and the principle of measurement was the same as for Futrex 5000. Our findings that NIRS data could accurately reflect fat mass are consistent with a previous study.[25] These results suggest that NIRS is a valid method for the estimation of AFM.

Other reports (by Futrex 5000) showed that NIRS might have little or no advantage over SFT in determining body composition.[32,33] One of the reasons for this controversy is that the degree of obesity differs in each patient. Elia *et al.* concluded that NIRS might underestimate body fat in very obese patients.[32] In the present study, the mean BMI of the patients was 23.3 ± 2.1 kg/m^2 in men and 22.6 ± 3.2 kg/m^2 in women, and there was no patient whose BMI was over 30 kg/m^2. Previous studies of older Japanese patients also reported a BMI ranging from 19.9 to 23.3 kg/m^2.[21,22] These results imply that NIRS data might be less affected by subcutaneous fat in older Japanese patients, and that NIRS is a valid method to assess their percentage fat and fat mass.

In contrast, NIRS data were not correlated significantly with whole and regional muscle mass except in the distal triceps. It is possible that quantitative assessment of skeletal muscle mass might be difficult using only NIRS data, because near infrared light might not reach the deeper muscle layer. However, when bodyweight is divided into fat mass and fat-free mass, skeletal muscle constitutes the largest fraction of appendicular fat-free mass. Previous investigators also proposed several models for predicting skeletal muscle mass with DXA. Lean body mass consists mostly of skeletal muscle. If we obtain an accurate bodyweight and the fat mass, the lean body weight (i.e. skeletal muscle mass) can be calculated automatically. The results in the present study suggest that AMM might be estimated indirectly by using NIRS data and bodyweight.

The present study is limited by the small sample size and orthopedic patients who were mostly women. The estimation equations of AMM and AFM developed in

the present study might have high specificity. In addition, we did not confirm the validity of these estimation equations. Thus, further studies are required to check the validity of these equations in other older adults (cross-validity) and longitudinally monitored populations (predictive validity) in the future. Furthermore, these equations will be developed for each sex using larger samples. Finally, to our knowledge, it is unclear whether the OD value (wavelength 937–947 nm) is influenced by blood flow and oxygen saturation. In the previous study, investigators did not mention this point. However, all patients were maintained in a resting position before and during the measurement in the present study. We think that the influence of blood flow and oxygen saturation is not likely to be marked, but this should be considered in a future study.

In conclusion, NIRS data can provide reliable and accurate estimates of AMM and AFM in older adults with the use of anthropometric data (height and weight). The estimation equations of AMM and AFM suggest the possibility that NIRS is a convenient method to assess body composition and to screen sarcopenic (or sarcopenic-obesity) patients. For further adjustment of this equation, it might be expected that sarcopenia or sarcopenic-obesity patients can be screened easily.

Acknowledgments

The present study was supported in part by a Health Labour Sciences Research Grant (Comprehensive Research on Aging and Health: H22-Choju-Ippan-002), Ministry of Health, Labour and Welfare, Japan. We thank the nursing staff in the Department of Orthopedic Surgery, National Hospital for Geriatric Medicine, National Center for Geriatric and Gerontology for their help in participant recruitment.

Disclosure statement

The authors have no financial disclosures or other conflicts of interest to report.

References

1 Baumgartner RN, Koehler KM, Gallagher D *et al.* Epidemiology of sarcopenia among the elderly in New Mexico. *Am J Epidemiol* 1998; **147**: 755–763.
2 Janssen I, Heymsfield SB, Ross R. Low relative skeletal muscle mass (sarcopenia) in older persons is associated with functional impairment and physical disability. *J Am Geriatr Soc* 2002; **50**: 889–896.
3 Janssen I, Baumgartner RN, Ross R, Rosenberg IH, Roubenoff R. Skeletal muscle cutpoints associated with elevated physical disability risk in older men and women. *Am J Epidemiol* 2004; **159**: 413–421.
4 Janssen I. Influence of sarcopenia on the development of physical disability: the Cardiovascular Health Study. *J Am Geriatr Soc* 2006; **54**: 56–62.
5 Janssen I. Evolution of sarcopenia research. *Appl Physiol Nutr Metab* 2010; **35**: 707–712.
6 Visser M, Goodpaster BH, Kritchevsky SB *et al.* Muscle mass, muscle strength, and muscle fat infiltration as predictors of incident mobility limitations in well-functioning older persons. *J Gerontol A Biol Sci Med Sci* 2005; **60**: 324–333.
7 Goodpaster BH, Park SW, Harris TB *et al.* The loss of skeletal muscle strength, mass, and quality in older adults: the health, aging and body composition study. *J Gerontol A Biol Sci Med Sci* 2006; **61**: 1059–1064.
8 Cosquéric G, Sebag A, Ducolombier C, Thomas C, Piette F, Weill-Engerer S. Sarcopenia is predictive of nosocomial infection in care of the elderly. *Br J Nutr* 2006; **96**: 895–901.
9 Miller MD, Crotty M, Giles LC *et al.* Corrected arm muscle area: an independent predictor of long-term mortality in community-dwelling older adults? *J Am Geriatr Soc* 2002; **50**: 1272–1277.
10 Baumgartner RN. Body composition in healthy aging. *Ann N Y Acad Sci* 2000; **904**: 437–448.
11 Morley JE, Baumgartner RN, Roubenoff R, Mayer J, Nair KS. Sarcopenia. *J Lab Clin Med* 2001; **137**: 231–243.
12 Baumgartner RN, Wayne SJ, Waters DL, Janssen I, Gallagher D, Morley JE. Sarcopenic obesity predicts instrumental activities of daily living disability in the elderly. *Obes Res* 2004; **12**: 1995–2004.
13 Rolland Y, Lauwers-Cances V, Cristini C *et al.* Difficulties with physical function associated with obesity, sarcopenia, and sarcopenic-obesity in community-dwelling elderly women: the EPIDOS (EPIDemiologie de l'OSteoporose) Study. *Am J Clin Nutr* 2009; **89**: 1895–1900.
14 Lee RC, Wang ZM, Heymsfield SB. Skeletal muscle mass and aging: regional and whole-body measurement methods. *Can J Appl Physiol* 2001; **26**: 102–122.
15 Visser M, Fuerst T, Lang T, Salamone L, Harris TB. Validity of fan-beam dual-energy X-ray absorptiometry for measuring fat-free mass and leg muscle mass. Health, Aging, and Body Composition Study – Dual-Energy X-ray Absorptiometry and Body Composition Working Group. *J Appl Physiol* 1999; **87**: 1513–1520.
16 Shih R, Wang Z, Heo M, Wang W, Heymsfield SB. Lower limb skeletal muscle mass: development of dual-energy X-ray absorptiometry prediction model. *J Appl Physiol* 2000; **89**: 1380–1386.
17 Tanimoto Y, Watanabe M, Higuchi Y, Hirota C, Kono K. Evaluation of the best indicator of muscle mass in community-dwelling elderly persons. *Nippon Ronen Igakkai Zasshi* 2008; **45**: 213–219.
18 Miyatani M, Kanehisa H, Fukunaga T. Validity of bioelectrical impedance and ultrasonographic methods for estimating the muscle volume of the upper arm. *Eur J Appl Physiol* 2000; **82**: 391–396.
19 Miyatani M, Kanehisa H, Masuo Y, Ito M, Fukunaga T. Validity of estimating limb muscle volume by bioelectrical impedance. *J Appl Physiol* 2001; **91**: 386–394.
20 Janssen I, Heymsfield SB, Baumgartner RN, Ross R. Estimation of skeletal muscle mass by bioelectrical impedance analysis. *J Appl Physiol* 2000; **89**: 465–471.
21 Yamada Y, Kimura M, Nakamura E, Masuo Y, Oda S. Limb muscle mass decrease with aging in Japanese men and women aged 15–97 yr. *Jpn J Phys Fitness Sports Med* 2007; **56**: 461–472. (In Japanese.)
22 Yamada Y, Schoeller DA, Nakamura E, Morimoto T, Kimura M, Oda S. Extracellular water may mask actual muscle atrophy during aging. *J Gerontol A Biol Sci Med Sci* 2010; **65**: 510–516.

23 Conway JM, Norris KH, Bodwell CE. A new approach for the estimation of body composition: infrared interactance. *Am J Clin Nutr* 1984; **40**: 1123–1130.
24 Sawai S, Shirayama M, Mutoh Y, Miyashita M. Estimation of body fat by near infrared spectroscopic technique. *Jpn J Phys Fitness Sports Med* 1990; **39**: 155–163. (In Japanese.)
25 Fuller NJ, Dewit O, Wells JC. The potential of near infrared interactance for predicting body composition in children. *Eur J Clin Nutr* 2001; **55**: 967–972.
26 Kim J, Wang Z, Heymsfield SB, Baumgartner RN, Gallagher D. Total-body skeletal muscle mass: estimation by a new dual-energy X-ray absorptiometry method. *Am J Clin Nutr* 2002; **76**: 378–383.
27 Chen Z, Wang Z, Lohman T *et al.* Dual-energy X-ray absorptiometry is a valid tool for assessing skeletal muscle mass in older women. *J Nutr* 2007; **137**: 2775–2780.
28 Kalantar-Zadeh K, Dunne E, Nixon K *et al.* Near infra-red interactance for nutritional assessment of dialysis patients. *Nephrol Dial Transplant* 1999; **14**: 169–175.
29 Sanada K, Miyachi M, Yamamoto K *et al.* Prediction models of sarcopenia in Japanese adult men and women. *Jpn J Phys Fitness Sports Med* 2010; **59**: 291–302. (In Japanese.)
30 Gallagher D, Visser M, De Meersman RE *et al.* Appendicular skeletal muscle mass: effects of age, gender, and ethnicity. *J Appl Physiol* 1997; **83**: 229–239.
31 Yasukawa M, Horvath SM, Oishi K, Kimura M, Williams R, Maeshima T. Total body fat estimations by near-infrared interactance, A-mode ultrasound, and underwater weighing. *Appl Human Sci* 1995; **14**: 183–189.
32 Elia M, Parkinson SA, Diaz E. Evaluation of near infra-red interactance as a method for predicting body composition. *Eur J Clin Nutr* 1990; **44**: 113–121.
33 Brooke-Wavell K, Jones PR, Norgan NG, Hardman AE. Evaluation of near infra-red interactance for assessment of subcutaneous and total body fat. *Eur J Clin Nutr* 1995; **49**: 57–65.

Geriatrics Gerontology 1st Impact Factor in June 2010 Medline Indexed

Geriatr Gerontol Int 2012

ORIGINAL ARTICLE

Relationship between near-infrared spectroscopy, and subcutaneous fat and muscle thickness measured by ultrasonography in Japanese community-dwelling elderly

Tatsuki Yoshimatsu,[1] Daisuke Yoshida,[2] Hiroyuki Shimada,[2] Taiki Komatsu,[1] Atsushi Harada[3] and Takao Suzuki[4]

[1]Department of Physical Therapy, School of Health Sciences, Tokyo University of Technology, Ota, Tokyo, [2]Section for Health Promotion, Department of Health and Medical Care, Center for Development of Advanced Medicine for Dementia, [3]Department of Orthopedic Surgery, National Hospital for Geriatric Medicine, National Center for Geriatric and Gerontology, and [4]Research Institute, National Center for Geriatrics and Gerontology, Obu, Aichi, Japan

Aim: Near-infrared spectroscopy (NIRS) allows estimation of the percentage of body fat (%BF) regardless of the patient's posture; thus, it is useful for assessment of elderly patients with severe decline of basic activity who cannot hold a standing position. However, the accuracy by which the near-infrared light emitted from NIRS reflects subcutaneous tissue is unknown. The aim of this study was to assess how correctly NIRS reflects the subcutaneous fat and muscle thickness derived from ultrasonography in community-dwelling elderly.

Methods: A total of 93 community-dwelling older adults aged 65 years and older were enrolled in this study (mean 75.8 years, 6.7 SD). Participants were assessed according to optical density (OD) measurements by NIRS, subcutaneous fat and muscle thickness by ultrasonography, and muscle strength. Pearson's correlation coefficients were calculated for each sex. Stepwise multiple regression analysis was used to identify factors that contributed to OD for each sex.

Results: OD measured at the forearm and thigh were significantly correlated with subcutaneous fat thickness. In stepwise multiple regression analyses, subcutaneous fat thickness was found to be a significant determinant of OD in men (forearm $\beta = -0.37$, $P = 0.01$; thigh $\beta = -0.63$, $P < 0.001$) and women (forearm $\beta = -0.50$, $P < 0.001$; thigh: $\beta = -0.52$, $P < 0.001$).

Conclusions: These results suggest that NIRS can appropriately estimate fat-free mass. By adding other variables to OD as the predictive variable, skeletal muscle mass might be estimated in the elderly population. **Geriatr Gerontol Int 2012; ••: ••–••.**

Keywords: near-infrared spectroscopy, older adults, sarcopenia, subcutaneous fat thickness, subcutaneous muscle thickness.

Introduction

Sarcopenia is the loss of muscle mass and function related to aging[1–5]. A study reported that older sarcopenic patients are twice as likely to contract infection during a hospital stay compared with older patients with a normal muscle mass.[6] This suggests that sarcopenic individuals might have decreased immunity, which might provide a mechanistic link between sarcopenia and mortality risk. In fact, a low corrected arm muscle area independently predicts long-term mortality in community-dwelling older adults.[7] According to the New Mexico Elder Health Survey, the prevalence of sarcopenia increased from 13% to 24% in persons aged less than 70 years to >50% in persons aged more than 80 years.[8] To achieve successful aging, it is important to preserve a certain amount of muscle mass.

Some researchers recently showed that sarcopenic obese persons are at a particularly high risk for functional impairment and physical disability.[8–11] A previous report suggested that approximately 15% of sarcopenic persons are also obese.[8] Thus, not only muscle mass, but also fat mass, should be accurately assessed in older adults.

Accepted for publication 16 May 2012.

Correspondence: Mr Tatsuki Yoshimatsu PhD, Department of Physical Therapy, School of Health Sciences, Tokyo University of Technology, 5-23-22 Nishi-kamata, Ota, Tokyo 144-8535, Japan. Email: yoshimatsu@hs.teu.ac.jp

doi: 10.1111/j.1447-0594.2012.00906.x

Protein energy malnutrition (PEM) is related to various risk factors (pressure sores, pneumonia, postoperative complications, anemia, loss of bone mineral, femoral neck fracture, cognitive impairment, low activities of daily living, low quality of life and sarcopenia).[12] Furthermore, PEM independently predicts long-term mortality in hospitalized older adults.[13] These individuals should have increased protein consumption, because energy uptake is insufficient in PEM; thus, the body protein (particularly in skeletal muscle) decreases. Therefore, sarcopenic patients might also have PEM. PEM has been reported to be prevalent in hospitalized older adults and nursing home residents,[14–16] whose physical functions often decrease severely. Therefore, body composition should be evaluated in patients with severe decline in physical function.

The most highly accurate method for measuring limb composition is whole-body dual-energy X-ray absorptiometry (DXA).[17] DXA can simultaneously measure body fat mass and bone mineral density. However, whole-body DXA is costly and time intensive. This scan also involves some exposure to radiation. Therefore, the use of bioelectrical impedance analysis (BIA) instruments has gained increasing attention both in the clinic and among the general population. However, few reports have been published about the measurement of body composition in lean elderly patients with severe decline in physical function.

BIA is a non-invasive, portable, quick and inexpensive method for measuring body composition.[18] It is the most common method for measuring body composition in Japan. However, many BIA instruments require patients to maintain a standing position for the measurement. Therefore, BIA instruments are often not used for elderly patients with severe decline in basic activity who cannot hold a standing position. Another method that might have potential for use in older adults is near-infrared spectroscopy (NIRS). NIRS is also a non-invasive, portable, simple and rapid method for assessing the percentage of body fat (%BF). The NIRS instrument allows estimating a patient's %BF simply by placing the tip of the probe against the center of the front side of the arm, regardless of the patient's posture.

Some reports showed that NIRS has a high reliability and accuracy in assessing %BF.[19–22] However, there has been no report on how correctly the near-infrared light emitted from NIRS reflects the subcutaneous tissue, particularly the muscle, at the irradiation point. Therefore, whether NIRS accurately estimates fat and muscle mass is unknown. Regional fat and muscle thickness can be accurately quantified with ultrasonography.[23,24] A previous study reported that the muscle cross-sectional area measured by ultrasonography is related to muscle strength.[25] If NIRS can reflect regional muscle mass, then there might be a relationship between the variable derived from NIRS and muscle strength.

The aim of the present study was to assess how correctly NIRS reflects the subcutaneous fat and muscle thickness derived from ultrasonography in community-dwelling older adults.

Methods

Participants

The participants were recruited from two volunteer databases (n = 1543), which included elderly individuals aged 65 years and older who were selected either by random sampling, or from those who attended a health check in Obu City near Nagoya in Japan. Among the 165 participants who responded to the eligibility assessments, 125 completed the strength, NIRS and ultrasound measurements. The inclusion criteria for the present study required that the participants be aged 65 years or older, living independently in the community, Japanese speaking, and with sufficient hearing and visual acuity to participate in the examinations. The exclusion criteria included a history of major psychiatric illness (e.g. schizophrenia or bipolar disorder), other serious neurological or musculoskeletal diagnoses, and clinical depression (Geriatric Depression Scale [GDS] score ≥10). A total of 93 out of 125 participants satisfied the inclusion criteria and were analyzed in the present study.

The present study was approved by the ethics committee of the National Center for Geriatrics and Gerontology. All participants provided written informed consent.

Near-infrared spectroscopy

The NIRS measurements used the Fitness Analyzer BFT-3000 (Kett Science, Tokyo, Japan), the Japanese version of Futrex 5000 (Futrex, Hagerstown, MD, USA), which can estimate body composition.[20,26] This device measures optical densities (OD) at two wavelengths (OD1 = 937 nm, OD2 = 947 nm). The NIRS instrument was tested immediately before obtaining measurements for each patient by using the optical standard provided with the instrument, which is situated in a flexible light shield to ensure its consistent performance throughout the study.

OD values were obtained at two sites: the forearm (flexor carpi radialis) and thigh (quadriceps). Participants were required to maintain a seated position, with their hands dropped to their sides. A single trained physical therapist carried out the NIRS measurements, which were completed in a few minutes.

Ultrasonography

The Miru Cube ultrasound scanning system (Global Healt, Kanagawa, Japan) with a 6-MHz linear array

transducer, a portable instrument developed for measuring subcutaneous fat and muscle thickness outside the clinic,[27] was used for measuring the thicknesses of two kinds of subcutaneous soft tissue: fat and muscle. Measurements were taken in longitudinal directions. Participants were required to maintain a seated position, with their hands dropped to their sides. Scans were taken at the same sites (forearm and thigh) as those in NIRS measurements. A single trained physical therapist carried out the scans, which were completed in a few minutes.

The images were transferred to a computer for quantification. Subcutaneous fat and muscle thicknesses were automatically measured using software for exclusive use.

Muscle strength

Grip strength and isometric knee-extension strength were evaluated. The grip strength was measured using a Smedley-type digital hand dynamometer (model TKK5401; Takei Scientific Instruments, Niigata, Japan). The participants were instructed to apply as much hand-grip pressure as possible with their dominant hand in a standing position.

Isometric knee-extension strength was tested on a dynamometer (model MDKKS; Molten, Hiroshima, Japan). For the knee extension test, the right leg was used unless contraindicated by pain or a history of joint replacement. Knee extension was measured while the participant was sitting (knee joint angle of 90°) on a chair by placing a strap around the leg just proximal to the ankle joint. In two experimental trials, the participant pulled against the strap assembly with maximal force; the greatest force was recorded. Isometric knee-extension torque was normalized against the moment arm and body mass (N m/kg) in the data analysis.

Statistical analysis

Student's *t*-tests were used to compare the demographic data, OD, subcutaneous soft tissue thicknesses, and muscle strengths between men and women.

Pearson's correlation coefficients were calculated for each sex to assess simple relationships between OD and subcutaneous soft tissue thicknesses or strengths. Stepwise multiple regression analysis was used to identify factors that contributed to OD for each sex and each measurement site (forearm or thigh). Because there were high correlation coefficients between OD1 and OD2 ($r > 0.969$) and all correlation coefficients were higher at OD1 than at OD2, OD1 was used as the representative value. For the analysis of variables measured in the forearm, OD1 in the forearm was considered the dependent variable, and subcutaneous soft tissue thicknesses in the forearm and grip strength were considered independent variables. For the analysis of variables measured in the thigh, OD1 in the thigh was considered the dependent variable, and subcutaneous soft tissue thicknesses in the thigh and knee-extension strength were considered independent variables.

We considered a value of 5% to be significant. We analyzed the data using IBM SPSS Statistics version 19 for Windows (SPSS, Chicago, IL, USA).

Results

The mean (SD) age of all participants was 75.8 years (6.7). Table 1 summarizes the characteristics and the sex differences of the participants.

The correlation coefficients between subcutaneous soft tissue thicknesses or strengths and each OD value are listed in Table 2. In both men and women, subcutaneous fat thickness in the forearm was significantly correlated with OD in the forearm or the thigh (both OD1 and OD2). In men, subcutaneous fat thickness in the thigh was significantly correlated with OD in the forearm or the thigh (both OD1 and OD2). In women, subcutaneous fat thickness in the thigh was significantly correlated with OD in the thigh (both OD1 and OD2). In men, knee-extension strength was significantly correlated with OD in the forearm (both OD1 and OD2). In the correlation analysis between subcutaneous fat thickness and OD value, all correlation coefficients were higher at OD1 than at OD2 (Figure 1).

In stepwise multiple regression analyses, subcutaneous fat thickness was found to be a significant determinant of OD1 in men (forearm $\beta = -0.37$, $P = 0.01$; thigh $\beta = -0.63$, $P < 0.001$) and women (forearm $\beta = -0.50$, $P < 0.001$; thigh $\beta = -0.52$, $P < 0.001$; Table 3).

Discussion

The power with which light enters the body is called penetrability. The penetrability of light is proportional to the wavelength. Electromagnetic waves with a short wavelength, such as visible light or near-infrared light, have low penetrability and can only warm the surface of the skin. The NIRS instrument used in the present study also measures the amount of subcutaneous soft tissue by means of such near-infrared light; thus, the light might not reach a deep subcutaneous point. A previous study reported that the deviation in optical path length in NIRS becomes large when there is a big difference in the skinfold thickness among participants.[28]

A previous study showed that the distances from the skin surface to muscle measured using an ultrasonography image scanner were 1.0–2.5 cm in participants whose body mass index was 20–24.[29] The NIRS instrument has been used to measure subcutaneous soft

Table 1 Participants' demographic information

Variables	Total $n = 93$	Men $n = 50$	Women $n = 43$	*P*-value
Age (years)	75.8 (6.7)	76.0 (6.5)	75.7 (6.9)	0.84
Height (cm)	154.6 (8.4)	159.9 (5.6)	148.4 (6.7)	<0.001
Weight (kg)	55.9 (8.7)	58.6 (7.8)	52.7 (8.6)	<0.001
BMI (kg/m^2)	23.3 (2.8)	22.9 (2.6)	23.8 (3.0)	0.10
OD (log1/I)				
Forearm				
OD1	1.090 (0.118)	1.138 (0.107)	1.036 (0.104)	<0.001
OD2	1.122 (0.108)	1.163 (0.099)	1.074 (0.096)	<0.001
Thigh				
OD1	1.036 (0.099)	1.059 (0.102)	1.010 (0.087)	0.01
OD2	1.100 (0.087)	1.114 (0.091)	1.084 (0.079)	0.10
Subcutaneous thicknesses (mm)				
Forearm				
Fat	4.7 (1.7)	4.4 (1.4)	5.0 (1.9)	0.09
Muscle	30.2 (3.0)	31.6 (2.4)	28.5 (2.7)	<0.001
Thigh				
Fat	6.6 (2.7)	5.8 (1.5)	7.5 (3.3)	<0.01
Muscle	18.9 (5.1)	18.7 (4.3)	19.0 (5.9)	0.75
Grip strength (kg)	25.6 (8.1)	30.8 (5.9)	19.6 (5.9)	<0.001
Knee-extension strength (N m/kg)	1.007 (0.381)	1.145 (0.347)	0.847 (0.356)	<0.001

Values are mean (SD). BMI, body mass index; OD, optical density; OD1, optical density at 937 nm; OD2, optical density at 947 nm.

Table 2 Correlation coefficients between subcutaneous thicknesses or strengths and each optical density value

	Forearm OD1	OD2	Thigh OD1	OD2
Men ($n = 50$)				
Subcutaneous thickness				
Fat in the forearm (mm)	−0.37**	−0.30*	−0.32*	−0.28*
Muscle in the forearm (mm)	−0.02	0.03	−0.01	0.04
Fat in the thigh (mm)	−0.38**	−0.35*	−0.63***	−0.58***
Muscle in the thigh (mm)	0.00	0.07	−0.05	−0.03
Grip strength (kg)	0.24	0.23	0.13	0.14
Knee-extension strength (N m/kg)	0.33*	0.35*	0.08	0.12
Women ($n = 43$)				
Subcutaneous thickness				
Fat in the forearm (mm)	−0.50***	−0.44**	−0.48**	−0.48**
Muscle in the forearm (mm)	−0.10	−0.08	−0.12	−0.09
Fat in the thigh (mm)	−0.28	−0.26	−0.51***	−0.45**
Muscle in the thigh (mm)	−0.25	−0.23	−0.12	−0.03
Grip strength (kg)	0.09	0.09	0.10	0.14
Knee-extension strength (N m/kg)	0.13	0.15	0.01	0.01

*$P < 0.05$, **$P < 0.01$, ***$P < 0.001$. OD, optical density; OD1, optical density at 937 nm, OD2, optical density at 947 nm.

tissue at a depth of 1.0–2.5 cm from the skin surface.[30] In the participants of the present study, the mean values of subcutaneous fat thickness were 7.2 mm (forearm of men), 8.8 mm (thigh of men), 8.8 mm (forearm of women), and 16.1 mm (thigh of women); the mean values of subcutaneous muscle thickness were 31.6 mm (forearm of men), 18.7 mm (thigh of men), 28.5 mm (forearm of women) and 19.0 mm (thigh of women).

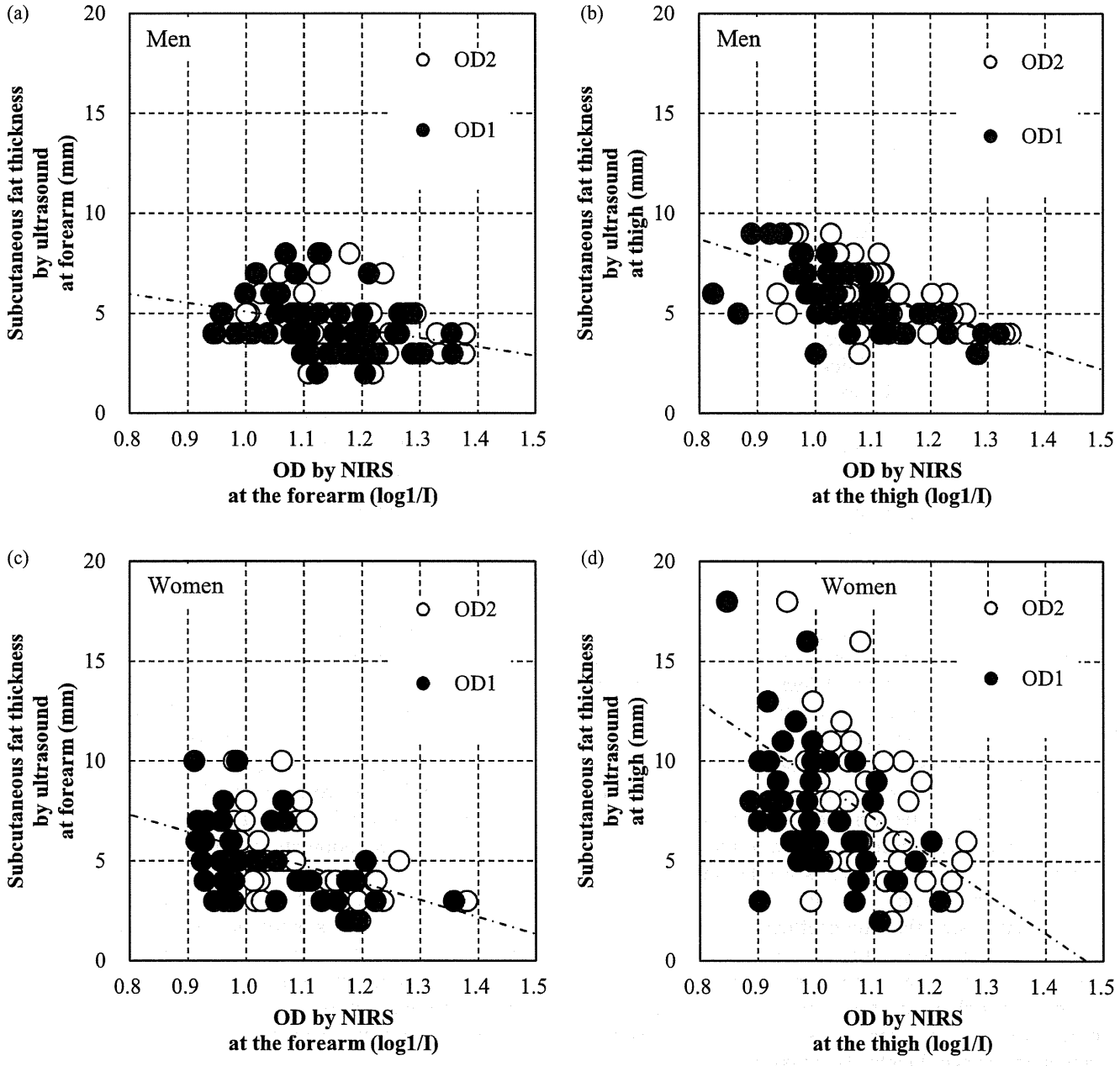

Figure 1 Scatter plot graphs showing the correlation between the subcutaneous fat thickness measured by ultrasound and the optical density (OD) from near-infrared spectroscopy (NIRS). (a,b) Data for men. (c,d) Data for women. Straight lines represent the regression line of OD at 937 nm (OD1), and broken lines represent the regression line of OD at 947 nm (OD2).

These results suggest that the near-infrared lights used in the present study did not reach the deepest point of the subcutaneous muscle layer of the participants. They also suggest that there was no significant correlation between OD and subcutaneous muscle thickness, although there were significant correlations between OD and subcutaneous fat thickness. In the stepwise multiple regression analysis, only subcutaneous fat thickness was included as a significant independent variable relevant to the OD value, and subcutaneous muscle thickness was excluded. Therefore, the estimation of muscle mass by NIRS is interpreted as lacking construct validity. However, this implies the opposite interpretation that the estimation of fat mass by NIRS has sufficient construct validity.

A two-component model dividing the human body into fat mass and fat-free mass is used when considering body composition at the molecular level.[31] This two-component model was the foundation of many methods for estimating body composition developed in the past. In this model, the construct validities for estimation of the fat mass and the fat-free mass are equally sufficient.

Table 3 Determinants of optical density at 937 nm in men and women

Independent variable	Men (n = 50)		Women (n = 43)	
	β	*P*-value	β	*P*-value
Forearm				
Entered				
Thickness of subcutaneous fat	−0.37	0.01	−0.50	<0.001
Removed				
Age	−1.33	0.19	−1.00	0.32
Thickness of subcutaneous muscle	−0.53	0.60	0.46	0.64
Grip strength	1.65	0.11	1.11	0.27
Thigh				
Entered				
Thickness of subcutaneous fat	−0.63	<0.001	−0.52	<0.001
Removed				
Age	−1.12	0.27	−0.62	0.54
Thickness of subcutaneous muscle	−0.02	0.99	−0.24	0.81
Knee-extension strength	0.79	0.43	0.33	0.74

Standardized beta values represent the correlation between optical density at 937 nm and each independent variable. OD, optical density; OD1, optical density at 937 nm.

Therefore, the results of the present study suggest that estimation of fat-free mass by using OD from NIRS has sufficient construct validity. When body composition is considered at the tissue level, the skeletal muscle is known to make up most of the fat-free mass.[31]

However, no significant correlation was found between OD and muscle strength in the present study. This suggests that the variable derived from NIRS is not the only index for estimating fat-free mass. A previous study has shown that there is a relationship between lean body mass and strength.[32] Furthermore, one report[33] suggested that the coefficient of determination became highest when the factors of maximum grip strength and physical performance were added as independent variables in the multiple linear regression model wherein lean mass was the dependent variable (adjusted for age, height, fat mass and activity) A high accuracy might be achieved if the muscle mass is determined by a multivariable estimation that includes OD plus physique indexes (such as height and fat mass), age and activity as independent variables.

To appropriately evaluate sarcopenia, it is ideal to directly measure the whole body skeletal muscle mass. However, it is very difficult to directly measure the body composition of a living human being; thus, an estimation is usually used. Because sarcopenia is related to critical risk factors, body composition needs to be estimated with high accuracy. If the body compositions of a population comprising various body forms are estimated from a single variable, great differences between the true values and the predicted values will be inevitable. Therefore, two or more variables should be used for estimation of body composition. For estimating body composition by using several variables, NIRS, which can appropriately estimate fat-free mass, might be an effective tool.

The present study was limited by all participants having a normal physique. In addition, we did not confirm the predictive validity, because the design of the present study was cross-sectional. Thus, the validity of the method should be confirmed by using longitudinally monitored populations including both thin and obese participants.

In conclusion, the OD value obtained by NIRS was strongly related to subcutaneous fat thickness. This result suggests that NIRS can appropriately estimate fat-free mass. If other variables are added to the OD as the predictive variable, skeletal muscle mass might be estimated with high accuracy in the elderly population.

Acknowledgments

This study was supported in part by a grant from the Japanese Ministry of Health, Labour and Welfare. We would like to thank the Obu City office for the help provided with regard to participant recruitment.

Disclosure statement

Source of support: Supported in part by the Ministry of Health, Labour and Welfare, Japan.

No commercial party having a direct financial interest in the results of the research supporting this article has or will confer a benefit on the authors or on any organization with which the authors are associated.

References

1 Baumgartner RN, Koehler KM, Gallagher D *et al.* Epidemiology of sarcopenia among the elderly in New Mexico. *Am J Epidemiol* 1998; **147**: 755–763.
2 Janssen I, Heymsfield SB, Ross R. Low relative skeletal muscle mass (sarcopenia) in older persons is associated with functional impairment and physical disability. *J Am Geriatr Soc* 2002; **50**: 889–896.
3 Janssen I, Baumgartner RN, Ross R, Rosenberg IH, Roubenoff R. Skeletal muscle cutpoints associated with elevated physical disability risk in older men and women. *Am J Epidemiol* 2004; **159**: 413–421.
4 Janssen I. Influence of sarcopenia on the development of physical disability: the Cardiovascular Health Study. *J Am Geriatr Soc* 2006; **54**: 56–62.
5 Janssen I. Evolution of sarcopenia research. *Appl Physiol Nutr Metab* 2010; **35**: 707–712.
6 Cosquéric G, Sebag A, Ducolombier C, Thomas C, Piette F, Weill-Engerer S. Sarcopenia is predictive of nosocomial infection in care of the elderly. *Br J Nutr* 2006; **96**: 895–901.
7 Miller MD, Crotty M, Giles LC *et al.* Corrected arm muscle area: an independent predictor of long-term mortality in community-dwelling older adults? *J Am Geriatr Soc* 2002; **50**: 1272–1277.
8 Baumgartner RN. Body composition in healthy aging. *Ann N Y Acad Sci* 2000; **904**: 437–448.
9 Morley JE, Baumgartner RN, Roubenoff R, Mayer J, Nair KS. Sarcopenia. *J Lab Clin Med* 2001; **137**: 231–243.
10 Baumgartner RN, Wayne SJ, Waters DL, Janssen I, Gallagher D, Morley JE. Sarcopenic obesity predicts instrumental activities of daily living disability in the elderly. *Obes Res* 2004; **12**: 1995–2004.
11 Rolland Y, Lauwers-Cances V, Cristini C *et al.* Difficulties with physical function associated with obesity, sarcopenia, and sarcopenic-obesity in community-dwelling elderly women: the EPIDOS (EPIDemiologie de l'OSteoporose) Study. *Am J Clin Nutr* 2009; **89**: 1895–1900.
12 Thomas DR, Ashmen W, Morley JE, Evans WJ. Nutritional management in long-term care: development of a clinical guideline. Council for Nutritional Strategies in Long-Term Care. *J Gerontol A Biol Sci Med Sci* 2000; **55**: M725–M734.
13 Coats KG, Morgan SL, Bartolucci AA, Weinsier RL. Hospital-associated malnutrition: a reevaluation 12 years later. *J Am Diet Assoc* 1993; **93**: 27–33.
14 Thomas DR, Verdery RB, Gardner L, Kant A, Lindsay J. A prospective study of outcome from protein-energy malnutrition in nursing home residents. *JPEN J Parenter Enteral Nutr* 1991; **15**: 400–404.
15 Abbasi AA, Rudman D. Observations on the prevalence of protein-calorie undernutrition in VA nursing homes. *J Am Geriatr Soc* 1993; **41**: 117–121.
16 Ferguson RP, O'Connor P, Crabtree B, Batchelor A, Mitchell J, Coppola D. Serum albumin and prealbumin as predictors of clinical outcomes of hospitalized elderly nursing home residents. *J Am Geriatr Soc* 1993; **41**: 545–549.
17 Cooper C, Dere W, Evans W *et al.* Frailty and sarcopenia: definitions and outcome parameters. *Osteoporos* 2012; **23**: 1839–1848.
18 Tanimoto Y, Watanabe M, Higuchi Y, Hirota C, Kono K. [Evaluation of the best indicator of muscle mass in community-dwelling elderly persons.] *Nippon Ronen Igakkai Zasshi* 2008; **45**: 213–219. (In Japanese.)
19 Conway JM, Norris KH, Bodwell CE. A new approach for the estimation of body composition: infrared interactance. *Am J Clin Nutr* 1984; **40**: 1123–1130.
20 Sawai S, Shirayama M, Mutoh Y, Miyashita M. [Estimation of body fat by near infrared spectroscopic technique. Jpn J Phys Fitness.] *Sports Med* 1990; **39**: 155–163. (In Japanese.)
21 Fuller NJ, Dewit O, Wells JC. The potential of near infrared interactance for predicting body composition in children. *Eur J Clin Nutr* 2001; **55**: 967–972.
22 Jensky-Squires NE, Dieli-Conwright CM, Rossuello A, Erceg DN, McCauley S, Schroeder ET. Validity and reliability of body composition analysers in children and adults. *Br J Nutr* 2008; **100**: 859–865.
23 Miyatani M, Kanehisa H, Ito M, Kawakami Y, Fukunaga T. The accuracy of volume estimates using ultrasound muscle thickness measurements in different muscle groups. *Eur J Appl Physiol* 2004; **91**: 264–272.
24 Kaneko H, Sato H, Maruyama H. [Reliability of lateral abdominal muscles thickness measurement using ultrasonography.] *Rigakuryoho Kagaku* 2005; **20**: 197–201. (In Japanese.)
25 Akagi R, Takai Y, Kato E *et al.* Relationships between muscle strength and indices of muscle cross-sectional area determined during maximal voluntary contraction in middle-aged and elderly individuals. *J Strength Cond Res* 2009; **23**: 1258–1262.
26 Kalantar-Zadeh K, Dunne E, Nixon K *et al.* Near infra-red interactance for nutritional assessment of dialysis patients. *Nephrol Dial Transplant* 1999; **14**: 169–175.
27 Fukuda O, Tsubai M, Sato T, Inoue M. [Development of an ultrasonographic device for healthcare.] *Jpn J Med Instrum* 2008; **78**: 113–124. (In Japanese.)
28 Hamaoka T, Katsumura T, Shimomitsu T *et al.* [Study on optical properties of the human forearm skeletal muscle.] *Ther Res* 1997; **18**: 148–152. (In Japanese.)
29 Sakai T, Osaki N, Yasuno F, Aikawa Y, Yano T. [Relations of stiff shoulders with deep hemodynamics values.] *J J A Phys M Baln Clim* 2002; **65**: 137–146. (In Japanese.)
30 Sakai A, Saito T. [Noninvasive continuous measurement of the oxygen consumption in the tissue using the near-infrared spectroscopy.] *Ther Res* 1995; **16**: 15–18. (In Japanese.)
31 Wang ZM, Pierson RN Jr, Heymsfield SB. The five-level model: a new approach to organizing body-composition research. *Am J Clin Nutr* 1992; **56**: 19–28.
32 Krause KE, McIntosh EI, Vallis LA. Sarcopenia and predictors of the fat free mass index in community-dwelling and assisted-living older men and women. *Gait Posture* 2011; **35**: 180–185.
33 Araujo AB, Chiu GR, Kupelian V *et al.* Lean mass, muscle strength, and physical function in a diverse population of men: a population-based cross-sectional study. *BMC Public Health* 2010; **10**: 508–516.